

# **Inductively Coupled Plasma/Optical Emission Spectrometry**

*Xiandeng Hou and Bradley T. Jones*

in

*Encyclopedia of Analytical Chemistry*

R.A. Meyers (Ed.)

pp. 9468–9485

© John Wiley & Sons Ltd, Chichester, 2000



# Inductively Coupled Plasma/Optical Emission Spectrometry

**Xiandeng Hou and Bradley T. Jones**

Wake Forest University, Winston-Salem, USA

<b>1</b>	<b>Introduction</b>	<b>1</b>
<b>2</b>	<b>Theory</b>	<b>2</b>
2.1	Inductively Coupled Plasma Operation	2
2.2	Inductively Coupled Plasma Characteristics	3
<b>3</b>	<b>Sample Introduction</b>	<b>3</b>
3.1	Nebulizers	4
3.2	Hydride Generation	5
3.3	Electrothermal Vaporization	6
3.4	Chromatographic Couplers	6
<b>4</b>	<b>Torch Configuration</b>	<b>7</b>
4.1	Radial View	7
4.2	Axial View	7
4.3	Dual View	7
<b>5</b>	<b>Detection of Emission</b>	<b>7</b>
5.1	Gratings	7
5.2	The Photomultiplier Tube	10
5.3	Array Detectors	11
5.4	Simultaneous Versus Sequential Detection	12
<b>6</b>	<b>Analytical Performance</b>	<b>12</b>
6.1	Analytical Wavelength	12
6.2	Analytical Figures of Merit	12
6.3	Interferences	14
	<b>Acknowledgments</b>	<b>15</b>
	<b>Abbreviations and Acronyms</b>	<b>15</b>
	<b>Related Articles</b>	<b>15</b>
	<b>References</b>	<b>16</b>

*Inductively coupled plasma/optical emission spectrometry (ICP/OES) is a powerful tool for the determination of metals in a variety of different sample matrices. With this technique, liquid samples are injected into a radiofrequency (RF)-induced argon plasma using one of a variety of nebulizers or sample introduction techniques. The sample mist reaching the plasma is quickly dried,*

*vaporized, and energized through collisional excitation at high temperature. The atomic emission emanating from the plasma is viewed in either a radial or axial configuration, collected with a lens or mirror, and imaged onto the entrance slit of a wavelength selection device. Single element measurements can be performed cost-effectively with a simple monochromator/photomultiplier tube (PMT) combination, and simultaneous multielement determinations are performed for up to 70 elements with the combination of a polychromator and an array detector. The analytical performance of such systems is competitive with most other inorganic analysis techniques, especially with regards to sample throughput and sensitivity.*

## 1 INTRODUCTION

ICP/OES is one of the most powerful and popular analytical tools for the determination of trace elements in a myriad of sample types (Table 1). The technique is based upon the spontaneous emission of photons from atoms and ions that have been excited in a RF discharge. Liquid and gas samples may be injected directly into the instrument, while solid samples require extraction or acid digestion so that the analytes will be present in a solution. The sample solution is converted to an aerosol and directed into the central channel of the plasma. At its core the inductively coupled plasma (ICP) sustains a temperature of approximately 10 000 K, so the aerosol is quickly vaporized. Analyte elements are liberated as free atoms in the gaseous state. Further collisional excitation within the plasma imparts additional energy to the atoms, promoting them to excited states. Sufficient energy is often available to convert the atoms to ions and subsequently promote the ions to excited states. Both the atomic and ionic excited state species may then relax to the ground state via the emission of a photon. These photons have characteristic energies that are determined by the quantized energy level structure for the atoms or ions. Thus the wavelength of the photons can be used to identify the elements from which they originated. The total number of photons is directly proportional to the concentration of the originating element in the sample.

The instrumentation associated with an ICP/OES system is relatively simple. A portion of the photons emitted by the ICP is collected with a lens or a concave mirror. This focusing optic forms an image of the ICP on the entrance aperture of a wavelength selection device such as a monochromator. The particular wavelength exiting the monochromator is converted to an electrical signal by a photodetector. The signal is amplified and processed by the detector electronics, then displayed and stored by a personal computer.

**Table 1** Survey of elemental application areas of ICP/OES<sup>(1-3)</sup>

Categories	Examples of samples
Agricultural and food	Animal tissues, beverages, feeds, fertilizers, garlic, nutrients, pesticides, plant materials, rice flour, soils, vegetables, wheat flour
Biological and clinical	Brain tissue, blood, bone, bovine liver, feces, fishes, milk powder, orchard leaves, pharmaceuticals, pollen, serum, urine
Geological	Coal, minerals, fossils, fossil fuel, ore, rocks, sediments, soils, water
Environmental and water	Brines, coal fly ash, drinking water, dust, mineral water, municipal wastewater, plating bath, sewage sludge, slags, seawater, soil
Metals	Alloys, aluminum, high-purity metals, iron, precious metals, solders, steel, tin
Organic	Adhesives, amino acids, antifreeze, combustion materials, cosmetics, cotton cellulose, dried wood, dyes, elastomers, epoxy, lubricant, organometallic, organophosphates, oils, organic solvent, polymers, sugars
Other materials	Acids, carbon, catalytic materials, electronics, fiber, film, packaging materials, paints and coatings, phosphates, semiconductors, superconducting materials

The characteristics of the ICP as an analytical atomic emission source are so impressive that virtually all other emission sources [such as the flame, microwave-induced plasma (MIP), direct current plasma (DCP), laser-induced plasma (LIP), and electrical discharge] have been relegated to specific, narrowly defined application niches. Indeed, even much of the application field originally assigned to atomic absorption spectrometry (AAS), using both the flame and graphite furnace atomic absorption spectrometry (GFAAS), has been relinquished to the ICP. Compared to these other techniques, ICP/OES enjoys a higher atomization temperature, a more inert environment, and the natural ability to provide simultaneous determinations for up to 70 elements. This makes the ICP less susceptible to matrix interferences, and better able to correct for them when they occur. In cases where sample volume is not limited, ICP/OES provides detection limits as low as, or lower than its best competitor, GFAAS, for all but a few elements. Even for these elements, the simplicity with which the ICP/OES instrument is operated often outweighs the loss in sensitivity.

## 2 THEORY

The ICP was developed for optical emission spectrometry (OES) by Fassel et al. at Iowa State University in the US and by Greenfield et al. at Albright & Wilson, Ltd. in the UK in the mid-1960s.<sup>(1,4,5)</sup> The first commercially available ICP/OES instrument was introduced in 1974. The ICP is now not only the most popular source for OES but it is also an excellent ion source for inductively coupled plasma mass spectrometry (ICPMS).<sup>(6)</sup> ICP/OES is a proven commercial success, and the future is still bright for ICP-based spectroscopic techniques. Detectability has been continuously and dramatically improved over the past 35 years. Detection limits, for

example, have improved by a factor of four to six orders of magnitude for many elements. Nevertheless, research and commercial opportunities for the further development of ICP/OES remain intriguing.<sup>(6)</sup>

### 2.1 Inductively Coupled Plasma Operation

As shown in Figure 1, the so-called ICP “torch” is usually an assembly of three concentric fused-silica tubes. These are frequently referred to as the outer, intermediate, and inner gas tubes. The diameter of the outer tube ranges from 9 to 27 mm. A water-cooled, two- or three-turn copper coil, called the load coil, surrounds the top section of the torch, and is connected to a RF generator. The outer argon flow (10–15 L min<sup>-1</sup>) sustains the high-temperature plasma, and positions the plasma relative to the outer walls and the induction coil, preventing the walls from melting and facilitating the observation of emission signals. The plasma under these conditions has an annular

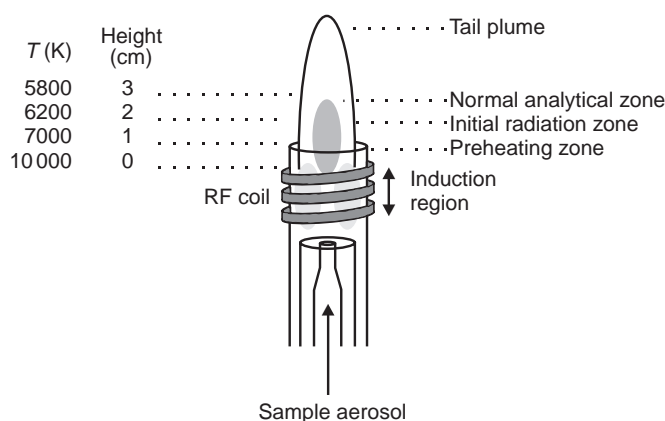


**Figure 1** Schematic diagram of an ICP assembly showing the three concentric tubes composing the torch, the RF coil, the different plasma regions, and the temperature as a function of height above the load coil.

shape. The sample aerosol carried by the inner argon flow ( $0.5\text{--}1.5\text{ L min}^{-1}$ ) enters the central channel of the plasma and helps to sustain the shape. The intermediate argon flow ( $0\text{--}1.5\text{ L min}^{-1}$ ) is optional and has the function of lifting the plasma slightly and diluting the inner gas flow in the presence of organic solvents.

The ICP is generated as follows. RF power, typically  $700\text{--}1500\text{ W}$ , is applied to the load coil and an alternating current oscillates inside the coil at a rate corresponding to the frequency of the RF generator. For most ICP/OES instruments, the RF generator has a frequency of either 27 or 40 MHz. The oscillation of the current at this high frequency causes the same high-frequency oscillation of electric and magnetic fields to be set up inside the top of the torch. With argon gas flowing through the torch, a spark from a Tesla coil is used to produce “seed” electrons and ions in the argon gas inside the load coil region. These ions and electrons are then accelerated by the magnetic field, and collide with other argon atoms, causing further ionization in a chain reaction manner. This process continues until a very intense, brilliant white, teardrop-shaped, high-temperature plasma is formed. Adding energy to the plasma via RF-induced collision is known as inductive coupling, and thus the plasma is called an ICP. The ICP is sustained within the torch as long as sufficient RF energy is applied.<sup>(1)</sup> In a cruder sense, the coupling of RF power to the plasma can be visualized as positively charged Ar ions in the plasma gas attempting to follow the negatively charged electrons flowing in the load coil as the flow changes direction 27 million times per second.

Figure 1 shows the temperature gradient within the ICP with respect to height above the load coil. It also gives the nomenclature for the different zones of the plasma as suggested by Koirtiyohann et al.<sup>(7)</sup> The induction region (IR) at the base of the plasma is “doughnut-shaped” as described above, and it is the region where the inductive energy transfer occurs. This is also the region of highest temperature and it is characterized by a bright continuum emission. From the IR upward towards the tail plume, the temperature decreases.

An aerosol, or very fine mist of liquid droplets, is generated from a liquid sample by the use of a nebulizer. The aerosol is carried into the center of the plasma by the argon gas flow through the IR. Upon entering the plasma, the droplets undergo three processes. The first step is desolvation, or the removal of the solvent from the droplets, resulting in microscopic solid particulates, or a dry aerosol. The second step is vaporization, or the decomposition of the particles into gaseous-state molecules. The third step is atomization, or the breaking of the gaseous molecules into atoms. These steps occur predominantly in the preheating zone (PHZ). Finally, excitation and ionization of the atoms occur, followed by the emission of radiation from these excited

species. These excitation and ionization processes occur predominantly in the initial radiation zone (IRZ), and the normal analytical zone (NAZ) from which analytical emission is usually collected.<sup>(1)</sup>

## 2.2 Inductively Coupled Plasma Characteristics

The main analytical advantages of the ICP over other excitation sources originate from its capability for efficient and reproducible vaporization, atomization, excitation, and ionization for a wide range of elements in various sample matrices. This is mainly due to the high temperature,  $6000\text{--}7000\text{ K}$ , in the observation zones of the ICP. This temperature is much higher than the maximum temperature of flames or furnaces ( $3300\text{ K}$ ). The high temperature of the ICP also makes it capable of exciting refractory elements, and renders it less prone to matrix interferences. Other electrical-discharge-based sources, such as alternating current and direct current arcs and sparks, and the MIP, also have high temperatures for excitation and ionization, but the ICP is typically less noisy and better able to handle liquid samples. In addition, the ICP is an electrodeless source, so there is no contamination from the impurities present in an electrode material. Furthermore, it is relatively easy to build an ICP assembly and it is inexpensive, compared to some other sources, such as a LIP. The following is a list of some of the most beneficial characteristics of the ICP source.

- high temperature ( $7000\text{--}8000\text{ K}$ )
- high electron density ( $10^{14}\text{--}10^{16}\text{ cm}^{-3}$ )
- appreciable degree of ionization for many elements
- simultaneous multielement capability (over 70 elements including P and S)
- low background emission, and relatively low chemical interference
- high stability leading to excellent accuracy and precision
- excellent detection limits for most elements ( $0.1\text{--}100\text{ ng mL}^{-1}$ )
- wide linear dynamic range (LDR) (four to six orders of magnitude)
- applicable to the refractory elements
- cost-effective analyses.

## 3 SAMPLE INTRODUCTION

A sample introduction system is used to transport a sample into the central channel of the ICP as either a gas, vapor, aerosol of fine droplets, or solid particles. The general requirements for an ideal sample introduction system include amenity to samples in all phases (solid, liquid, or gas), tolerance to complex matrices, the ability

to analyze very small amount of samples (<1 mL or <50 mg), excellent stability and reproducibility, high transport efficiency, simplicity, and low cost.<sup>(2)</sup> A wide variety of sample introduction methods have been developed, such as nebulization, hydride generation (HG), electrothermal vaporization (ETV), and laser ablation.<sup>(1,8,9)</sup>

### 3.1 Nebulizers

Nebulizers are the most commonly used devices for solution sample introduction in ICP/OES. With a nebulizer, the sample liquid is converted into an aerosol and transported to the plasma. Both pneumatic and ultrasonic nebulizers (USNs) have been successfully used in ICP/OES. Pneumatic nebulizers make use of high-speed gas flows to create an aerosol, while the USN breaks liquid samples into a fine aerosol by the ultrasonic oscillations of a piezoelectric crystal. The formation of aerosol by the USN is therefore independent of the gas flow rate.

Only very fine droplets (about 8 μm in diameter) in the aerosol are suitable for injection into the plasma. A spray chamber is placed between the nebulizer and the ICP torch to remove large droplets from the aerosol and to dampen pulses that may occur during nebulization. Thermally stabilized spray chambers are sometimes adopted to decrease the amount of liquid introduced into the plasma, thus providing stability especially when organic solvents are involved. Pneumatic nebulization is very inefficient, however, because only a very small fraction (less than 5%) of the aspirated sample solution actually reaches the plasma. Most of the liquid is lost down the drain in the spray chamber. However, the pneumatic nebulizer retains its popularity owing to its convenience, reasonable stability, and ease of use. Efficiency may only be a concern when sample volumes are limited, or measurements must be performed at or near the detection limit.

Three types of pneumatic nebulizers are commonly employed in ICP/OES: the concentric nebulizer, the cross-flow nebulizer, and the Babington nebulizer (Figure 2). The concentric nebulizer is fashioned from fused silica. Sample solution is pumped into the back end of the nebulizer by a peristaltic pump. Liquid uptake rates may be as high as 4 mL min<sup>-1</sup>, but lower flows are more common. The sample solution flows through the inner capillary of the nebulizer. This capillary is tapered so that flexible tubing from the pump is attached at the entrance (4 mm outer diameter) and the exit has a narrow orifice approaching 100 μm or less in inner diameter. Ar gas (0.5–1.5 L min<sup>-1</sup>) is supplied at a right angle into the outer tube. This tube is also tapered so that the exit internal diameter approaches the outer diameter

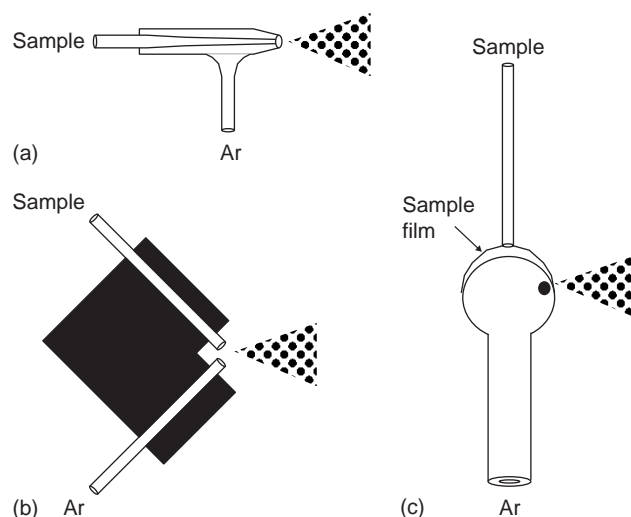


**Figure 2** Schematic diagrams of three types of pneumatic nebulizer: (a) the concentric nebulizer; (b) the cross-flow nebulizer; and (c) the Babington nebulizer.

for the sample capillary. As the Ar passes through this narrow orifice, its velocity is greatly increased, resulting in the shearing of the sample stream into tiny droplets. Concentric nebulizers have the advantages of excellent sensitivity and stability, but the small fragile fused-silica orifices are prone to clogging, especially when aspirating samples of high salt content. Concentric nebulizers also require a fairly large volume of sample, given the high uptake rate. The microconcentric nebulizer (MCN) is designed to solve this problem. The sample uptake rate for the MCN is less than 0.1 mL min<sup>-1</sup>. The compact MCN employs a smaller diameter capillary (polyimide or Teflon<sup>®</sup>) and poly(vinylidene difluoride) body to minimize the formation of large droplets and to facilitate the use of hydrofluoric acid.

A second type of pneumatic nebulizer, the cross-flow nebulizer, is designed to reduce the clogging problem. In contrast to concentric nebulizers, cross-flow nebulizers use a high-speed stream of argon perpendicular to the tip of the sample capillary. Again the sample solution is broken into an aerosol, as shown in Figure 2. The drawbacks of the cross-flow nebulizer include lower sensitivity and potential capillary misalignment.

The third type of pneumatic nebulizer used for ICP/OES is the Babington nebulizer that allows a film of the sample solution to flow over a smooth surface having a small orifice (Figure 2).<sup>(10)</sup> High-speed argon gas emanating from the hole shears the sheet of liquid into small droplets. The essential feature of this type of nebulizer is that the sample solution flows freely over a small aperture, rather than passing through a fine capillary, resulting in a high tolerance to dissolved solids.

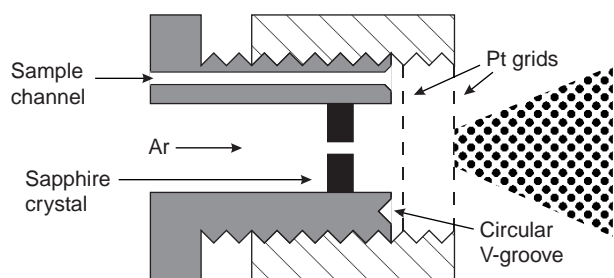


**Figure 3** The HGN.

In fact, even slurries can be nebulized with a Babington nebulizer. This type of nebulizer is the least susceptible to clogging and it can nebulize very viscous liquids.<sup>(1)</sup>

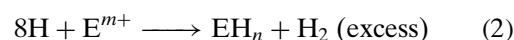
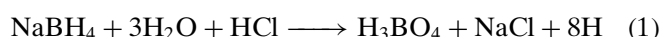
The Hildebrandt grid nebulizer (HGN) (Figure 3) may be considered a specialized version of the Babington nebulizer with many orifices. Often the nebulizer has a screw-cap design. The outer member (cap) of the nebulizer holds two parallel platinum screens or grids. The grids are separated by approximately 2 mm. The inner body of the nebulizer (screw) has a single sample channel. Liquid is pumped through this channel at rates up to  $1 \text{ mL min}^{-1}$ . The inner body also has a circular V-groove that allows the liquid to contact the entire perimeter of the inner platinum grid. In this fashion, the liquid completely wets both grids. A high-velocity stream of argon ( $1 \text{ L min}^{-1}$ ) blows through the center of the nebulizer. Often the velocity of the argon is increased by placing a sapphire crystal containing a small orifice (0.2 mm) in the center of the gas stream. The high-velocity argon forces the liquid through the tiny openings in the screens producing a fine aerosol. The HGN is characterized by clog-free operation, high efficiency, and excellent stability.

With the USN, sample solution is first introduced onto the surface of a piezoelectric transducer that is operated at a frequency between 0.2 and 10 MHz. The longitudinal wave, which is propagated in the direction perpendicular to the surface of the transducer towards the liquid-air interface, produces pressure that breaks the liquid into an aerosol.<sup>(11)</sup> The efficiency of an USN is typically between 10 and 20%. This nebulizing efficiency is greater than that of a pneumatic nebulizer, and it is independent of argon flow rate. Therefore, a slower gas flow rate can be used to transport the aerosol to the plasma, thus prolonging the residence time of analyte in the plasma. This results in improved sensitivity, and the limit of detection (LOD) is usually lowered by a factor of 8–200, depending upon the element. However, the USN is more complicated, more expensive, and more susceptible to matrix effects, memory effects, and high solid loading. The USN is not compatible with hydrofluoric acid. Various other means

of nebulization have been tested with limited degrees of success.<sup>(11)</sup>

### 3.2 Hydride Generation

HG is a very effective sample introduction technique for some elements. These elements include arsenic, bismuth, germanium, lead, antimony, selenium, tin, and tellurium. In this method, the sample in diluted acid solution is mixed with a reducing agent, usually a solution of sodium borohydride in dilute sodium hydroxide. The reaction of sodium borohydride with the acid produces hydrogen. The hydrogen then reduces the analyte metal ions to hydrides, which are gaseous at ambient temperatures. The chemical reactions are shown in Equations (1) and (2).



where E is the hydride forming element of interest and  $m$  may or may not equal  $n$ .

The advantages of the HG technique include:

- physical separation of the analyte from possible matrix interferences;
- higher efficiency than conventional pneumatic nebulization;
- preconcentration of the analyte for better LOD;
- capability for inorganic and/or organic speciation;
- ease of automation when used with flow injection techniques.

On the other hand, several disadvantages of this technique may include:

- interference from those contaminants that reduce HG efficiency;
- slow reactions, necessitating hydride trapping prior to introduction;

**Table 2** LOD observed by hydride generating, HG/ICP/OES<sup>(1,8)</sup>

Elements	LOD by HG ( $\text{ng mL}^{-1}$ )	LOD by conventional nebulization ( $\text{ng mL}^{-1}$ )	Ratios (conventional/HG)
As	0.03	20	667
Bi	0.06	20	333
Ge	0.3	20	67
Pb	1.0	10	10
Sb	0.07	10	143
Se	0.04	50	1250
Sn	0.2	30	150
Te	0.04	10	250

- critical control of experimental conditions such as pH and reagent concentrations;
- extra influential factors, such as the oxidation state of the analyte of interest.

LODs for the hydride generating elements are listed in Table 2, together with those observed for conventional nebulization techniques. The LODs of HG/ICP/OES in Table 2 are the best LOD cited in Nakahara's review paper.<sup>(8)</sup> Compared with conventional pneumatic nebulization techniques, LODs achieved by the HG technique are enhanced by a factor between 10 and 1000, depending upon the element.

### 3.3 Electrothermal Vaporization

ETV has also been used to solve problems associated with pneumatic nebulization. Graphite furnaces or other electrothermal devices, such as carbon rods, carbon cups, graphite boats, graphite tubes, tungsten wire, and other metal filaments, have been used in research laboratories to electrothermally vaporize a liquid or solid sample for introduction into the ICP.<sup>(12)</sup> Other vaporization methods, such as arc/spark vaporization and laser ablation/vaporization, have also been used as means for sample introduction in ICP/OES. Even the ICP itself has been used to vaporize samples into a second ICP for analytical measurements.<sup>(13)</sup> In a typical experiment, a low current is applied to the ETV to remove the sample solvent. A small portion of the sample is then vaporized by the device through the application of a high current. An optional "ash" step may be used to remove some of the matrix prior to the analyte vaporization step. The resulting dense cloud of the analyte vapor is then efficiently swept into the center of the plasma by a flow of argon gas.

A commercial graphite furnace designed for AAS is most frequently used in ETV/ICP/OES. The major advantage of ETV as a means of sample introduction is that the transportation efficiency is dramatically improved over a pneumatic nebulizer, from less than 5% to over 60%. Consequently, the LODs are improved by at least an order of magnitude. Some difficult to analyze samples, those with high total dissolved solids (TDS) for example, can be introduced by the ETV. However, since these devices are generally not of a continuous-flow nature, the ICP instrument has to be capable of recording transient signals. Also, the simultaneous multielement capability of the system could be limited due to this transient nature of signals. Furthermore, when graphite material is used for the ETV, carbide formation could be a problem for some elements, resulting in lowered sensitivity and memory effects for refractory elements.

In an attempt to eliminate the problems associated with graphite, metal filaments have been employed for

ETV/ICP/OES. For example, a tungsten coil from a commercial slide projector bulb can be used to vaporize liquid samples prior to their introduction into the ICP.<sup>(12)</sup> A small volume, typically 20  $\mu$ L, of sample solution is delivered to the tungsten coil and dried at low current. Then, a higher current is applied to atomize the sample from the coil. The vapor is then rapidly introduced into the plasma as a dense plug by a flow of argon/hydrogen gas. The LOD is typically improved by 100–1500 times compared with pneumatic nebulization. These LODs are comparable to those obtained by GFAAS, but with the capability of simultaneous multielement measurement, and at a low cost. A tungsten loop has also been used as an in-torch vaporization (ITV) means for sample introduction to the ICP, and the operation can possibly be automated.<sup>(14)</sup> These approaches still share some of the other disadvantages associated with graphite furnace ETV, and commercial systems have not yet appeared.

### 3.4 Chromatographic Couplers

The combination of the separation power of chromatography and the detection power of atomic emission spectroscopy results in many advantages. One of the primary advantages of chromatography over conventional sample introduction is the ability to obtain speciation information.<sup>(15)</sup> When used as a detector for chromatographic methods, the ICP offers good sensitivity, wide LDR and multielement detection capability. The multielement capability of ICP, in turn, enhances the performance of chromatographic methods. Both gas chromatography (GC) and high-performance liquid chromatography (HPLC) can be coupled with ICP/OES.<sup>(16)</sup> Compared with HPLC, however, the GC/ICP coupling is less common because the analytical performance of ICP/OES for nonmetals is often not adequate. Undoubtedly, GC/ICP/OES is still useful in the analyses of volatile organometallics, as demonstrated in the determination of methylmercury species.<sup>(17)</sup> The successful combination of these two techniques is realized through the use of chromatographic couplers. Fortunately, most of the interface systems currently in use are relatively inexpensive and easy to construct, and they require few, if any, modifications to commercial ICP/OES instruments.

Direct connections between the end of the HPLC column and the nebulizer suffer from poor transport efficiency and low tolerance to many of the organic solvents commonly employed in mobile phases for HPLC, particularly when a pneumatic nebulizer is used. To improve the transport efficiency and to minimize the influence of organic solvents on the stability of the ICP, USNs, water-cooled thermospray chambers, and glass-frit nebulizers have been utilized for sample introduction in HPLC/ICP/OES. The solvent load on the plasma can



also be decreased by aerosol thermostating, increasing the incident RF power, application of a condenser, or by use of a micro-HPLC column.

Other major sample introduction methods, such as thermospray, direct sample insertion, and laser ablation, have also been used for ICP/OES.<sup>(18–20)</sup> Each of these has its advantages and disadvantages. For example, laser ablation can be used to vaporize any solid samples into the ICP, but generally it has poor reproducibility and high cost.

## 4 TORCH CONFIGURATION

The atomic emission from the NAZ, as shown in Figure 1, is sampled for spectrometric measurements. Two configurations may be employed for observing emission from the ICP. One is referred to as a radial or side-on viewing of the plasma, and the other is known as an axial or end-on viewing of the plasma. A third viewing mode is the combination of these two basic modes, and is known as dual view. These are all commercially available, and each of them has advantages and disadvantages.

### 4.1 Radial View

The radial view is the classical operation mode for ICP/OES. With radial viewing, the plasma is operated in a vertical orientation, and the analytical zone is observed from the side of the plasma. Radial viewing constrains the observation volume in the NAZ, and thus limits the effect of potential spectral and background interferences.

### 4.2 Axial View

With the axial view, the plasma is rotated to a horizontal position and the NAZ of the ICP is observed from the end of the plasma. The axial view provides better LODs than radial view.<sup>(21)</sup> This may be attributed to the longer viewing path available down the axis of the plasma. Thus, a better sensitivity and a 5- to 10-fold improvement in the LOD can be achieved. The disadvantages of the axial view include the increased potential for spectral interference and matrix-induced interferences. Moreover, self-absorption effects can be quite severe because the observations are made through the much cooler tail plume of the plasma. These effects can be significantly reduced by use of a shear gas.<sup>(22)</sup> The shear gas displaces the tail plume from the optical path, and thus reduces the self-absorption. Spectral interferences may be either corrected or minimized by improving spectral resolution, using an alternate analytical line with less or no interference, or by applying an interelement correction (IEC) factor.<sup>(1)</sup>

## 4.3 Dual View

In cases of very complicated sample matrices having a wide range of elemental concentrations, the axial view may be inappropriate. Recent commercial instruments combine the axial view and radial view configurations into a single unit, known as dual view. This dual view system allows the user to optimize the appropriate configuration for the type of sample without the expense of two separate ICP/OES systems.<sup>(1)</sup>

## 5 DETECTION OF EMISSION

### 5.1 Gratings

ICP/OES is characterized by remarkably rich spectra. For example, the 70 elements most commonly determined by the technique give rise to at least 70 000 total emission lines in the 200–600 nm wavelength range. A consequence of this high density of spectral information is the need for high resolving power. The low-resolution dispersive systems typically employed with atomic absorption spectrometers will not suffice. Spectral interferences will occur in this case if only a small number of elements are present at moderate concentrations in the sample. Much higher resolution is desirable in ICP/OES, with spectral bandpass ( $\Delta\lambda_s$ ) 0.01 nm or lower if possible. Traditionally, this degree of resolution has been accomplished using plane grating monochromators with large focal lengths ( $f = 0.5$  m or more).

Figure 4 depicts a plane ruled grating. The normal to the grating surface (N) is shown as a dashed line. A light ray incident to the grating approaches at angle  $\alpha$  measured with respect to N. The diffracted ray leaves the grating surface at angle  $\beta$ . Parallel rays striking the grating on different adjacent groove facets will travel

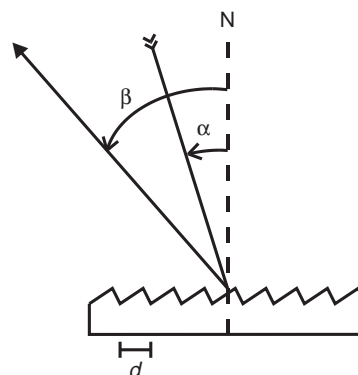


**Figure 4** Diagram of the plane-ruled grating. N is the normal to the grating surface,  $\alpha$  is the angle of incidence measured with respect to N, and  $\beta$  is the angle of diffraction measured with respect to N.  $d$  is the width of a single groove.

a different distance before reaching a common position beyond the grating. If the difference in distance traveled is a multiple of the wavelength of the light incident upon the grating surface, then the rays will undergo constructive interference. Otherwise, destructive interference will occur. Relatively simple geometrical considerations result in the grating formula shown in Equation (3):

$$d(\sin \alpha + \sin \beta) = m\lambda \quad (3)$$

This equation shows the relationship between  $\alpha$ ,  $\beta$ , the groove spacing ( $d$ ), the wavelength of light ( $\lambda$ ) and the order of diffraction ( $m$ ). The order of diffraction may take any integer value including zero. At zero order, all wavelengths undergo constructive interference at the same diffraction angle. In the first order, one particular wavelength will undergo constructive interference at the angle  $\beta$  that corresponds to the specular reflection angle for rays incident at angle  $\alpha$ . This wavelength is called the blaze wavelength for the grating, and it is determined by the angle at which the grooves are cut with respect to the surface of the grating. A grating is most efficient at its blaze wavelength. Typically a grating may have an efficiency as high as 70% at its blaze wavelength, so the intensity measured at the blaze wavelength will be 70% of the intensity that would be measured at the specular reflectance angle for a polished mirror of the same coating and material as the grating.

Normally, when a plane grating is employed, the angle of incidence is nearly 0, so  $\sin \alpha$  approaches 0. In this case, the grating formula may be further reduced, as shown in Equation (4):

$$\sin \beta = \frac{m\lambda}{d} \quad (4)$$

The angular dispersion of the grating ( $d\beta/d\lambda$ ) may be found, as shown in Equations (5) and (6), by taking the derivative of both sides of the above equation with respect to  $\lambda$ :

$$(\cos \beta) \frac{d\beta}{d\lambda} = \frac{m}{d} \quad (5)$$

$$\frac{d\beta}{d\lambda} = \frac{m}{d \cos \beta} \quad (6)$$

The angular dispersion therefore increases with larger order, smaller groove spacing, or larger  $\beta$ . Angular dispersion may be converted to linear dispersion along the exit focal plane of the monochromator by simply multiplying by the focal length ( $f$ ) of the monochromator. The spectral bandpass ( $\Delta\lambda_s$ ) in wavelength units is then determined by dividing the slit width of the monochromator by the linear dispersion. So  $\Delta\lambda_s$  gets smaller (higher resolution) for larger  $f$ , larger order, larger  $\beta$ , smaller  $d$ , and smaller slit width. A typical

plane grating is operated in the first order. The groove density of the grating might be as high as 3600 grooves per millimeter, so the groove spacing ( $d$ ) might be as small as 0.0003 mm. Therefore, assuming  $\beta$  is  $45^\circ$  and the slit width is  $25 \mu\text{m}$ , a monochromator with a focal length of 500 mm will provide a spectral bandpass of 0.01 nm. Such a system will effectively isolate most ICP emission lines. Simultaneous multielement determinations are not performed effectively with such a system however. The focal plane for this type of monochromator is 5 cm long at best, so the entire spectral window will be approximately 20 nm in width. Unless the analytes of interest exhibit emission lines within 20 nm of one another, the wavelength must be scanned to detect multiple elements. So two other optical approaches have become more popular for simultaneous determinations: the concave grating placed on a Rowland circle, and the echelle grating coupled with a prism order-sorting device.

Shortly after designing his grating ruling engine in 1881, Rowland first conceived the idea of ruling gratings on a spherical mirror of speculum metal.<sup>(23)</sup> The most important property of such a concave grating was also observed by Rowland. If the source of light and the grating are placed on the circumference of a circle, and the circle has a diameter equal to the radius of curvature of the grating, then the spectrum will always be brought to a focus on the circle. Hence the focal “plane” is curved, and of considerable length (Figure 5). In this case one entrance slit is placed on the circle for introduction of the source radiation, and multiple exit slits may be placed around the circle at the analytical wavelengths of interest. Hence Rowland’s circle is ideally suited for multielement

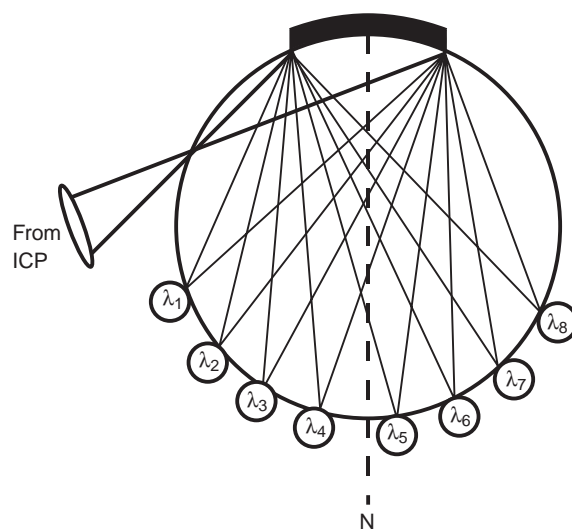


**Figure 5** The Paschen–Runge mounting of a concave grating on a Rowland circle. The grating, entrance slit, and focused images of the diffracted wavelengths are all positioned on the perimeter of the circle. N is the grating normal.

ICP emission spectrometry. A further advantage of the Rowland geometry is the elimination of the need for any collimating or focusing lenses or mirrors. A Rowland circle spectrometer with same groove density, slit width, and focal length as the plane grating system described above will provide similar spectral bandpass but with a much larger spectral window.

The echelle grating is a coarsely ruled grating, typically having a groove density of 70 grooves per millimeter, so  $d = 0.014$  mm. The increase in spectral bandpass due to the increase in  $d$  is overcome by operating the grating in higher orders ( $m = 25$  to 125), and by using steeper angles of diffraction ( $\beta > 45^\circ$ ). Figure 6 demonstrates how the steeper side of the groove facets are used with the echelle grating. If the steep sides of the grooves are blazed such that specular reflectance occurs when  $\alpha = 60^\circ$  and  $\beta = 50^\circ$ , then each wavelength will exhibit a peak in grating efficiency at a particular order as determined by the grating formula. For example, for the 70 grooves per millimeter grating described above, the order of maximum efficiency ( $m_{\max}$ ) occurs as shown in Table 3. The efficiency of the grating for a given wavelength at its optimum order can be as high as 65%. This level of efficiency is typically attained across the free spectral range for a given order. The free spectral range ( $\Delta\lambda_f$ ) is defined as the range of wavelengths over which no overlap from adjacent orders occurs, and is given by Equation (7):

$$\Delta\lambda_f = \frac{\lambda}{m + 1} \quad (7)$$

As indicated in Table 3,  $\Delta\lambda_f$  is very small for large values of  $m$ . Obviously, then, severe spectral overlap occurs with an echelle grating. The overlap does not simply

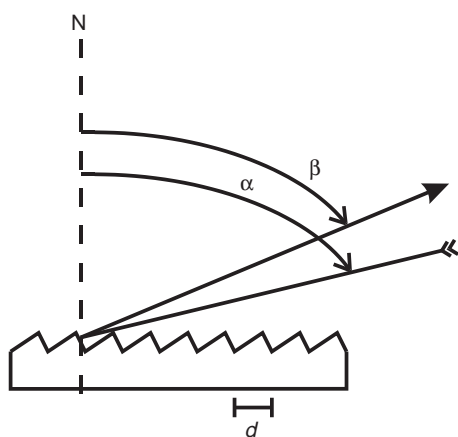


**Figure 6** Diagram of the echelle grating.  $N$  is the normal to the grating surface,  $\alpha$  is the angle of incidence measured with respect to  $N$ , and  $\beta$  is the angle of diffraction measured with respect to  $N$ . The light is incident to the steeper sides of the groove facets, and approaches the grating at nearly grazing angles ( $62^\circ$ ).  $d$  is the width of a single groove.

**Table 3** The order of maximum efficiency and the free spectral range at that order for an echelle grating having 70 grooves per millimeter, angle of incidence ( $\alpha$ ) of  $60^\circ$ , and blaze angle ( $\beta$ ) of  $50^\circ$

$\lambda$ (nm)	$m_{\max}$	$\Delta\lambda_f$ (nm)
200	117	1.7
250	93	2.7
300	78	3.8
350	67	5.2
400	58	6.7

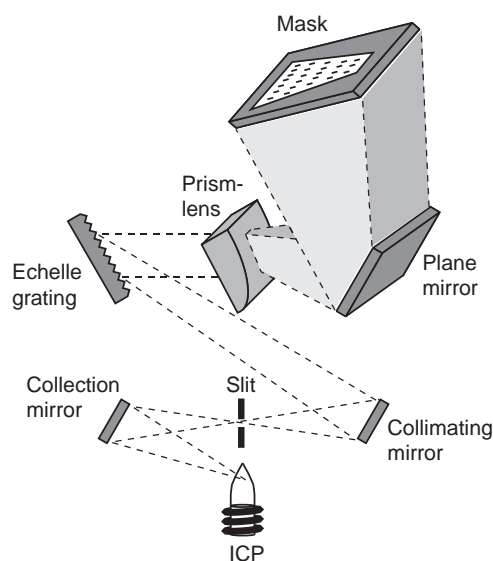


**Figure 7** Schematic diagram of an echelle polychromator. (Adapted from the schematic diagram of the DRE/ICP provided by Leeman Labs, Inc., Hudson, NH.)

involve adjacent orders, but all orders are dispersed in multiple layers along the same focal plane. This overlap is corrected most often with an order-sorting prism. This prism is placed between the echelle grating and the focal plane (Figure 7). The prism is positioned so that it disperses the light in a direction perpendicular to the direction of dispersion of the grating. As a result, the focal plane has wavelength dispersed in the horizontal direction and order sorted in the vertical direction. The free spectral range (and the region of maximum efficiency) has a roughly triangular shape centered horizontally on the plane (Figure 8). An echelle monochromator often provides a spectral bandpass nearly 10 times smaller than that of a typical grating monochromator with a similar focal length. In addition, the echelle system provides high efficiency at many wavelengths rather than a single blaze wavelength. Finally, both the high efficiency and superior resolution are available over a very broad spectral window.

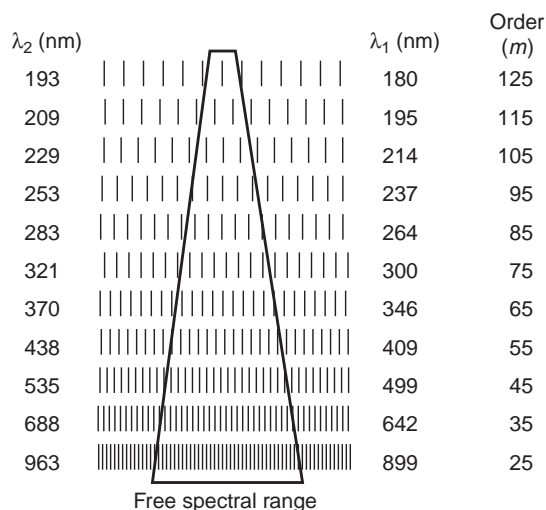


**Figure 8** The two-dimensional focal plane provided by the echelle polychromator. The triangle-shaped free spectral range is the region of highest grating efficiency. The distance between adjacent vertical lines is 1 nm, and the beginning ( $\lambda_1$ ) and ending ( $\lambda_2$ ) wavelengths depicted by the lines are listed for each order. Only one out of every 10 orders is shown for clarity.

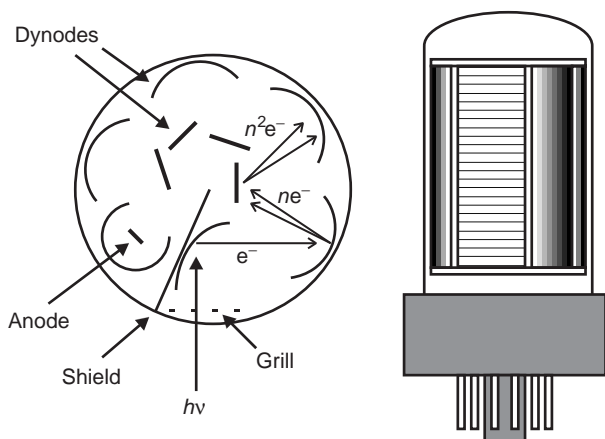


**Figure 9** Cross-sectional and front views of a side-on PMT. In the cross-section, two types of dynodes are depicted: curved (outer) and flat (inner). The outside surfaces of the curved dynodes are seen in the front view.

## 5.2 The Photomultiplier Tube

Figure 9 is a schematic representation of the PMT. Like its predecessor, the vacuum phototube, the heart of the PMT consists of two electrodes sealed in a fused-silica envelope. The cathode has a relatively large surface area, usually in the shape of a vertical, hollow “half cylinder”. The cathode is made from a photoemissive material such as an alkali metal oxide. The anode is simply an electron collection wire or grid. Unlike the phototube, however, the PMT has up to 14 secondary emission dynodes placed between the cathode and the anode. Typically the anode is

fixed to ground potential and the dynodes are at potentials that are successively more negative, by about 100 V per dynode. The potential of the cathode is typically  $-1000$  V.

A photon generated in the ICP and passing through the wavelength selection device may pass through the fused silica envelope of the PMT, through a baffle-type grill, and strike the photocathode. If the energy of the photon is higher than the work function of the photocathode material, then an electron may be ejected from the cathode. The fraction of photons with energy greater than the work function that actually produce a photoelectron is called the quantum efficiency of the photocathode. The quantum efficiency may be as high as 0.5, and it depends upon the photocathode material and upon wavelength. A plot of quantum efficiency versus wavelength is called the spectral response curve for the PMT. The spectral response curve is usually supplied by the manufacturer.

Once an electron has been ejected by the photocathode, it is accelerated towards the first dynode. Upon impact, the first dynode releases  $x$  secondary electrons (where  $x$  is typically between 2 and 5). This process continues at each dynode, with each electron impact imparting  $x$  new secondary electrons. So by the time that the pulse generated by a single photon reaches the anode it has been greatly multiplied, hence the name “multiplier” phototube or PMT. The gain,  $G$ , for a PMT can be defined as shown in Equation (8):

$$G = x^n \quad (8)$$

where  $n$  is the number of dynodes. The gain depends upon the voltage across the PMT and it may be as high as  $10^8$ . One of the best features of the PMT is that the gain is acquired with almost no increase in noise. Thus the PMT is ideally suited for the detection of small analytical signals against a relatively dark background, as is the case near the detection limit in high resolution atomic emission spectrometry.

Usually the entrance aperture as defined by the grill on the PMT is very large compared to a single resolution element at the focal plane of a monochromator. This disparity is corrected by placing a mechanical slit on the focal plane in front of the PMT. The width of this slit then defines the range of wavelengths ( $\Delta\lambda_s$ ) that is allowed to strike the PMT. Sequential detection of multiple elements can be accomplished by changing the grating angle in a conventional monochromator and thus scanning the wavelengths that are detected. A second approach is to move the PMT rapidly along the focal curve of a Rowland circle spectrometer. Such a spectrometer may have several pre-aligned exit slits along the focal curve, each corresponding to a particular element (Figure 5). A still more efficient method for sequential multielement determinations involves the

echelle polychromator (Figure 7). A mask with many slits, each corresponding to a different element, is placed upon the two-dimensional focal plane. The PMT is held in a mechanical arm that quickly positions the detector at the appropriate  $x$ - $y$  coordinates for a given element. This design allows very fast sequential determinations by “wavelength hopping” or direct reading rather than scanning linearly through all wavelengths to reach a select few. One commercial instrument using this design is called a Direct Reading Echelle (DRE) ICP instrument.

Simultaneous multielement determinations may be performed with multiple PMTs, but such designs quickly become limited by the size of the PMTs and the geometry of the polychromator. Multiple PMTs may be positioned either along the focal curve of a Rowland circle spectrometer or along the exit plane of an echelle polychromator. Solid-state detectors, with their relatively small size and their intrinsic multielement nature, are usually more effective for simultaneous determinations.

### 5.3 Array Detectors

Charge transfer devices (CTDs) include a broad range of solid-state silicon-based array detectors.<sup>(24)</sup> They include the charge injection device (CID) and the charge-coupled device (CCD). The CCD has found extensive use in nonspectroscopic devices such as video cameras, bar code scanners, and photocopiers. With the CTDs, photons falling on a silicon substrate produce electron–hole pairs. The positive electron holes migrate freely through the p-type silicon semiconductor material, while the electrons are collected and stored temporarily by an array of metal oxide semiconductor (MOS) capacitors (Figure 10). Each MOS capacitor is composed of a small metal electrode and a thin layer of insulating  $\text{SiO}_2$  material on top of the p-type silicon substrate. A positive potential is applied to the metal electrode, so the electrons generated in a given region are trapped just below the insulating layer. Each MOS capacitor (or pixel) has a width in the 5- to 50- $\mu\text{m}$  range, and a height that may be as large

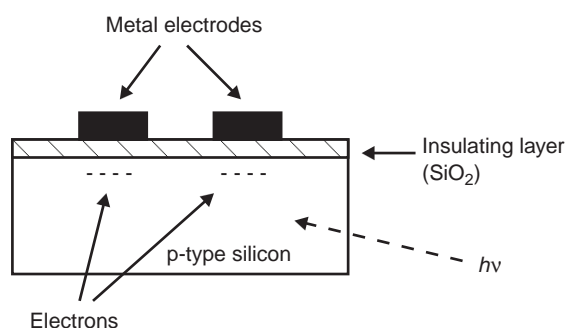


**Figure 10** Cross-sectional diagram of two adjacent pixels in a CCD detector.

as 200  $\mu\text{m}$ . A two-dimensional array of pixels is easily prepared by proper placement of the metal electrodes. Such arrays may vary in size up to 4096 pixels on an edge. The CCD differs from the CID mainly in the readout scheme. The CCD is read out in a sequential charge shifting manner towards the output amplifier. The CID on the other hand may be read out in a nondestructive manner by shifting charge between adjacent electrodes, and then shifting it back again. The CID thus benefits from quick random access, even during long integration periods.

Spectroscopic applications of CTDs has been hampered by the physical mismatch between the relatively small surface area of the detector and the large sometimes two-dimensional focal plane associated with polychromators. This mismatch may be overcome, however, and one commercial ICP spectrometer employs a CID detector having more than 250 000 pixels positioned upon an echelle focal plane.

Alternative approaches have been successful with the CCD detector. In one case, a group of several CCD arrays are arranged around a Circular Optical System (CIROS) based upon a Rowland circle design. Rather than monitoring discrete wavelengths as is the case with the multiple PMT Rowland circle systems, the CIROS system provides total wavelength coverage from 120 to 800 nm, with resolution on the order of 0.009 nm.

A second multiple CCD array detector has become very popular commercially. This detector, called a segmented array charge-coupled device detector (SCD), employs over 200 small subarrays of 20–80 pixels each.<sup>(24)</sup> The subarrays are positioned along the two-dimensional focal plane of an echelle polychromator. The position of each subarray corresponds to one of the 236 most prominent ICP emission lines of the most commonly determined 70 ICP elements. This design allows for discrete wavelength determinations as seen with the multiple PMT designs, but it also provides additional spectral information around the vicinity of each emission line without exhaustively recording data at all wavelengths.

Another approach to correcting the mismatch between conventional imaging CCD arrays and the focal plane of an echelle spectrometer, is to specifically design a CCD array to exactly match the spectrometer image.<sup>(25)</sup> This process, called image-mapping the detector, has recently been accomplished and is available commercially in the form of the VistaChip. The VistaChip consists of a series of 70 diagonalized linear arrays (DLAs) of pixels that are designed to exactly match the individual diffraction orders present in the focal plane of the echelle spectrometer. The 70 DLAs correspond to orders 19–88, and the length of an individual DLA is set to match the free spectral range for the corresponding order. In this fashion, continuous wavelength coverage is provided

across the range 167–363 nm, and selected coverage is provided in the range 363–784 nm where the diffraction orders are wider than the selected width of the detector (although no atomic emission lines of relevance miss the detector). The overall dimensions of the VistaChip are 15 by 19 mm, and a total of 70 908 pixels are packed inside the 70 DLAs.

#### 5.4 Simultaneous Versus Sequential Detection

In the final analysis, the detection system most appropriate for an ICP emission system depends upon the application. In cases where only one or two elements will be determined routinely, the traditional scanning sequential detection system may be sufficient. The high sensitivity provided by a PMT coupled with the flexibility of interrogating any wavelength region may outweigh the need for rapid determinations. On the other hand, if the application may vary between the determination of a few elements to the determination of many, the reasonable cost and high sensitivity of the PMT-based direct reading systems may be attractive. Finally, if a large suite of elements must be determined on a routine basis, one of the array-based detection systems might be most suitable.

## 6 ANALYTICAL PERFORMANCE

### 6.1 Analytical Wavelength

The ultraviolet and visible regions (160–800 nm) of the electromagnetic spectrum are most commonly used for analytical atomic spectrometry. In ICP/OES, the number of elements that can be determined is related to the wavelength window that can be covered by both the collimating and the dispersive optical system. Wavelengths above 500 nm should be used when alkali metals need to be determined, whereas wavelengths below 190 nm or even below 160 nm should be used when elements such as chlorine, bromine, nitrogen, arsenic must be determined. Spectral overlap must also be kept in mind in the selection of analytical lines. There are several criteria for selecting analytical lines. First, the wavelengths must be accessible by both the dispersive system and the detector. Second, the wavelengths must exhibit signal levels appropriate for the

concentrations of the respective elements in the sample. Third, the wavelengths selected must be free from spectral interferences. When this is not possible, emission lines whose intensities can be corrected to account for spectral interferences should be chosen. Fourth, if an internal standard scheme is used, it may be preferable to match the analyte ion lines with an internal standard ion line, and analyte neutral atom lines with an internal standard neutral atom line.

### 6.2 Analytical Figures of Merit

For ICP/OES, the analytical figures of merit include the number of elements that can be determined, selectivity, reproducibility, long-term stability, susceptibility to matrix interferences, LOD, and accuracy.<sup>(26)</sup> The number of elements that can be measured by ICP/OES is often more than 70 out of a total of 92 naturally occurring elements, as listed in Table 4. Routine determination of 70 elements can be accomplished by ICP/OES at concentration levels below 1 mg L<sup>-1</sup>. As can be seen from Table 4, almost all naturally occurring elements, with the exception of hydrogen, oxygen, fluorine, and inert gases, can be determined by ICP/OES. The elements that are not usually determined by ICP/OES fall into three basic categories. The first category includes those elements that occur either as trace contaminants in the argon gas used in the ICP/OES (C from CO<sub>2</sub>), constituents of the sample solvent (C, O, H), or as contaminants from the environment or atmosphere (N for example). The second category encompasses those elements that require high excitation energy, such as the halogens. These elements could be determined with poor LOD, however. The third category is the family of short-lived radioactive elements that are commonly determined by  $\gamma$ -ray spectrometry.<sup>(1)</sup>

Selectivity is important to minimize the spectral overlap interferences resulting from elements with rich line-emission spectra (tungsten, cobalt, niobium, molybdenum, tantalum, and rear earth elements) and to improve the signal-to-background ratio (SBR).<sup>(26)</sup> Selectivity is largely decided by the practical resolution of the wavelength dispersive system of the ICP/OES instrument. High selectivity is usually achieved with a sacrifice in sensitivity and the wavelength coverage range. For the best commercial ICP/OES instruments, a resolution of less than 5 pm is possible.<sup>(26)</sup>

**Table 4** A list of elements that can be determined by ICP/OES

Alkaline and alkaline earth	Rare earth	Transition metal	Others
Li, Na, K, Rb, Cs, Be, Mg, Ca, Sr, Ba	Ce, Pr, Nd, Sm, Eu, Gd, Tb, Dy, Ho, Er, Tm, Yb, Lu, Th, U	Sc, V, Ti, Cr, Mn, Fe, Co, Ni, Cu, Zn, Y, Nb, Zr, Mo, Ru, Th, Pd, Ag, Cd, La, Hf, Ta, W, Re, Os, Ir, Pt, Au, Hg	B, C, N, Al, Si, P, S, Cl, Ga, Ge, As, Se, Br, In, Sn, Sb, Te, I, Tl, Pb, Bi

The LODs of ICP/OES are generally in the nanogram per milliliter range. The LOD is usually defined as the analyte concentration that produces an analytical signal equivalent to three times the standard deviation observed for 16 measurements of a blank solution.<sup>(27)</sup> Another definition for the LOD of ICP/OES is related to the SBR of the analyte line at a given concentration,  $c$ , and the relative standard deviation (RSD) of the background,  $RSD_B$  as shown in Equation (9):<sup>(28)</sup>

$$\text{LOD} = \frac{3 \times c \times \text{RSD}_B}{\text{SBR}} \quad (9)$$

The LOD is determined, therefore, by the sensitivity of the measurement and the noise level, or stability, of the ICP/OES instrument. The high degree of stability of an ICP was identified when Greenfield et al.<sup>(5)</sup> first used an ICP for analytical atomic spectrometry. For the best ICP/OES instruments, a long-term stability of less than 1% RSD has been achieved.<sup>(26)</sup> The atomic emission signals from the ICP are larger than those from other sources, such as a flame. This occurs because the high-temperature and inert-argon environment of the

**Table 5** LOD ( $\mu\text{g L}^{-1}$ ) observed for ICP/OES with different nebulizers and different viewing modes<sup>(1,3)</sup>

Element	HGN <sup>(3)</sup>	USN <sup>(3)</sup>	Ratio (HGN/USN)	Radial view <sup>(1)</sup>	Axial view <sup>(3)</sup>
Ag	6.1	0.71	9	1	0.6
Al	10.5	3.85	3	3	1.9
As	12.8	2.05	6	20	3.8
B	7.4	NA	NA	1	NA
Ba	0.28	0.11	3	0.1	0.12
Be	0.11	0.04	3	0.1	0.09
Ca	14.5	1.38	11	0.02	NA
Cd	1.3	0.59	2	1	0.2
Co	1.7	0.56	3	1	0.8
Cr	1.6	0.49	3	2	0.4
Cu	1.8	0.50	4	0.4	0.7
Fe	2.5	0.38	7	2	0.5
K	152	17.39	8	20	5
Li	4	0.40	10	0.3	NA
Mg	24.8	6.65	4	0.1	NA
Mn	0.61	0.09	7	0.4	0.07
Mo	2.2	0.58	4	3	0.8
Na	11.7	2.23	5	3	2.2
Ni	3.9	1.66	2	5	1.6
P	34.2	9.44	4	30	NA
Pb	10.7	1.60	7	10	1.6
Sb	15.6	2.65	6	10	2.6
Se	23	2.03	11	50	3.8
Si	14.3	3.48	4	4	NA
Sn	8.6	0.90	10	30	NA
Sr	0.3	0.05	6	0.06	NA
Ti	0.65	0.17	4	0.5	NA
Tl	14.2	2.05	7	30	4.8
V	2.8	0.41	7	0.5	0.4
Zn	1.5	0.40	4	1	0.4

**Table 6** LODs (pg) for ETV/ICP/OES compared with those of GFAAS<sup>(2,31,32)</sup>

Elements	ETV/ICP/OES	GFAAS
Ag	1	0.5
Al	0.5	4
As	60	20
Au	10	10
Ba	0.3	10
Be	1	1
Bi	200	10
B	4	NA
Ca	150	5
Cd	1	0.3
Co	12	1
Cu	2	1
Er	34	300
Eu	12	10
Fe	10	2
Ga	10	10
Ge	10	20
Hg	4	100
In	20	5
K	1200	2
Li	2	5
Lu	54	4000
Mg	0.1	0.4
Mn	0.3	1
Mo	7	4
Na	400	5
Ni	27	10
P	100	3000
Pb	4	5
Pt	25	50
Rb	2800	5
Re	100	NA
Ru	95	40
Sb	100	20
Sc	17	40
Se	450	20
Si	100	40
Sn	20	20
Sr	5	2
Te	50	10
Ti	6	100
Tl	300	10
U	3	2.4 $\mu\text{g}$
V	6	20
W	160	NA
Y	25	NA
Yb	18	4
Zn	0.6	1

NA, not available.

ICP leads to more efficient atomization, ionization, and excitation. In fact, the temperature of the ICP is so high that the largest signals are usually from the ionic lines. There are many other factors that may influence LOD, such as nebulizer type, view mode, and sample matrix.<sup>(29,30)</sup> Table 5 shows ICP/OES LODs obtained for various nebulizers and different viewing modes.

LODs using an axially viewed plasma are typically better than those observed by radial viewing by a factor of 5–10,<sup>(1)</sup> and this is even true for instruments from different manufacturers, as shown in Table 5. Table 6 shows LODs for ETV/ICP/OES in comparison with those of GFAAS. LODs for many elements by ETV/ICP/OES are better than or equivalent to those achieved by GFAAS.<sup>(31,32)</sup> Notice that some elements that cannot be determined by GFAAS can be measured by ICP/OES.

Often the background equivalent concentration (BEC) is also used to check instrumental performance in ICP/OES. The BEC is defined as the concentration of a solution that results in an analyte emission signal equivalent in intensity to that of the background emission signal at the measurement wavelength. The BEC can be used as an indicator of relative sensitivity for an emission line. An unusually high BEC often indicates problems with the efficiency of the sample introduction system.

The LDR of calibration curves for ICP/OES is usually four to six orders of magnitude wide, starting from the LOD on the low concentration side. These LDRs are significantly larger than the two to three orders of magnitude observed for competing techniques such as AAS and arc/spark OES. The wide LDRs in ICP/OES translate into simple preparation of calibration curves. Very often a single standard together with a blank is enough to produce an accurate curve. Multiple sample dilutions are seldom needed prior to the analysis.

In general, the accuracy of the ICP/OES technique gets poorer as the analyte concentration approaches the LOD. For semiquantitative analysis (accuracy  $\pm 10\%$ ) the analyte concentration should be at least five times higher than the LOD. For accurate quantitation ( $\pm 2\%$ ), the concentration should be 100 times greater than the LOD. At this concentration level, the precision is typically better than 1% RSD. This precision is considered sufficient for most trace element determinations. Better precision can be achieved, if necessary, by sacrificing analysis speed or with a more complex instrumental design. Recently, the concept of limit of quantitation (LOQ) has been defined as a concentration for which the precision, expressed as RSD, would be below a given threshold, for instance 10% or 5%.<sup>(33)</sup> A 5%-based LOQ would normally occur at concentrations approximately 10 times greater than the LOD (based upon three standard deviations).

### 6.3 Interferences

Among all commonly used analytical atomic spectrometry techniques, ICP/OES is probably the one with the fewest interferences. The argon plasma is inert when compared to the chemical reactivity of a flame. Also, the high temperature of the plasma helps to reduce chemical

interferences. The temperature is high enough to break down most species into atoms or ions for excitation and subsequent emission. In contrast, in a low temperature flame, chemical interferences can be a severe problem. For example, a small amount of aluminum will interfere with the determination of calcium in flame AAS, but even at aluminum concentration 100 times higher than this, interference is not observed in ICP/OES. However, chemical interferences do exist in the ICP. Sometimes higher RF power and/or lower inner argon flow rates are used to reduce these interferences. One particular type of chemical interference is the so-called easily ionized element (EIE) effect. The EIEs are those elements that have low ionization potentials, such as alkaline elements. High concentrations of EIEs can suppress or enhance emission signals, depending upon the analyte species. One way to reduce the EIE effect is to dilute the sample solution to the point that the EIE effect is not measurable. Sometimes, higher RF power or mathematical correction may be used to compensate for EIE interference. Instrumental conditions such as observation width, viewing height, and viewing volume can be chosen to minimize such interference and to optimize emission signal collection in either axial or radial configuration.<sup>(34)</sup>

The most common interference problem in ICP/OES is spectral interference (also referred to as background interference). Ironically, this type of interference arises because of the multielement nature of the plasma. Since the ICP is capable of exciting almost any element that is introduced into the plasma, spectra are likely to be rich especially for highly complex and concentrated samples. The solution to the spectral interference problem, as discussed previously, is the use of high-resolution spectrometers. Some spectral overlap may even exist with the best commercial system. In these cases advanced background correction techniques are employed or a different analytical wavelength for the element(s) of interest is chosen. Spectral interferences can be categorized into four categories: simple background shift, sloping background shift, direct spectral overlap, and complex background shift. The simple background shift is defined as a shift in background intensity that is essentially constant over a given wavelength range on either side of the analytical line. The background may shift up or down. There are two approaches to deal with this background problem. The first is to select a different analytical line at a wavelength with no background interference. The second is to correct for the background by measuring it somewhere near, but not falling on, the profile of the analytical line of the analyte element. Two background correction points, one on each side of the profile of the analytical line, are used to correct for the sloping background shift. This means that the average signal measured at the two points is subtracted from the total



signal measured at the analytical line. In the worst case, direct spectral overlap occurs. This can be corrected if the magnitude of the interference is known as a function of the concentration of the interfering element. A correction factor can be calculated and used to correct the signal measured at the analyte wavelength. This can be best achieved by making simultaneous measurements of both the signal at the analyte wavelength and at a different wavelength for the interfering element. This method is referred to as the concentration ratio method or IEC. The basic requirement is that the concentration of the interfering element can be accurately measured at another wavelength. With advanced detector systems, all spectral lines are present, so IEC is possible. A complex background shift is a shift in a background intensity that varies significantly on both sides of the analytical line. This is usually caused by the occurrence of a number of intense, closely spaced emission lines nearby, and perhaps directly overlapping the analyte wavelength. In this case, a different analytical wavelength should be chosen if possible.<sup>(1)</sup>

## ACKNOWLEDGMENTS

The authors acknowledge that the preparation of the manuscript was partially done in Professor Robert G. Michel's research laboratory, and are grateful for access to all the facilities for the writing of this article. This work was funded in part by a grant from the National Science Foundation GOALI program (CHE-9710218).

## ABBREVIATIONS AND ACRONYMS

AAS	Atomic Absorption Spectrometry
BEC	Background Equivalent Concentration
CCD	Charge-coupled Device
CID	Charge Injection Device
CIROS	Circular Optical System
CTD	Charge Transfer Device
DCP	Direct Current Plasma
DLA	Diagonalized Linear Array
DRE	Direct Reading Echelle
EIE	Easily Ionized Element
ETV	Electrothermal Vaporization
GC	Gas Chromatography
GFAAS	Graphite Furnace Atomic Absorption Spectrometry
HG	Hydride Generation
HGN	Hildebrand Grid Nebulizer
HPLC	High-performance Liquid Chromatography

ICP	Inductively Coupled Plasma
ICPMS	Inductively Coupled Plasma Mass Spectrometry
ICP/OES	Inductively Coupled Plasma/Optical Emission Spectrometry
IEC	Interelement Correction
IR	Induction Region
IRZ	Initial Radiation Zone
ITV	In-torch Vaporization
LDR	Linear Dynamic Range
LIP	Laser-induced Plasma
LOD	Limit of Detection
LOQ	Limit of Quantitation
MCN	Microconcentric Nebulizer
MIP	Microwave-induced Plasma
MOS	Metal Oxide Semiconductor
NAZ	Normal Analytical Zone
OES	Optical Emission Spectrometry
PHZ	Preheating Zone
PMT	Photomultiplier Tube
RF	Radiofrequency
RSD	Relative Standard Deviation
SBR	Signal-to-background Ratio
SCD	Segmented Array Charge-coupled Device Detector
TDS	Total Dissolved Solids
USN	Ultrasonic Nebulizer

## RELATED ARTICLES

*Clinical Chemistry (Volume 2)*  
Atomic Spectrometry in Clinical Chemistry

*Coatings (Volume 2)*  
Atomic Spectroscopy in Coatings Analysis

*Environment: Trace Gas Monitoring (Volume 3)*  
Laser-induced Breakdown Spectroscopy, Elemental Analysis

*Environment: Water and Waste (Volume 3)*  
Environmental Analysis of Water and Waste: Introduction • Atomic Fluorescence in Environmental Analysis • Capillary Electrophoresis Coupled to Inductively Coupled Plasma-Mass Spectrometry for Elemental Speciation Analysis • Flame and Graphite Furnace Atomic Absorption Spectrometry in Environmental Analysis • Gas Chromatography with Atomic Emission Detection in Environmental Analysis • Heavy Metals Analysis in Seawater and Brines • Hydride Generation Sample Introduction for Spectroscopic Analysis in Environmental Samples • Inductively Coupled Plasma Mass Spectrometry in Environmental Analysis

**Environment: Water and Waste cont'd (Volume 4)**

Laser Ablation Inductively Coupled Plasma Spectrometry in Environmental Analysis • Microwave-assisted Techniques for Sample Preparation in Organic Environmental Analysis • Optical Emission Inductively Coupled Plasma in Environmental Analysis • Sample Preparation for Elemental Analysis of Biological Samples in the Environment • Sample Preparation for Environmental Analysis in Solids (Soils, Sediments, and Sludges) • Sample Preparation Techniques for Elemental Analysis in Aqueous Matrices • Sampling Considerations for Biomonitoring

**Food (Volume 5)**

Atomic Spectroscopy in Food Analysis

**Forensic Science (Volume 5)**

Atomic Spectroscopy for Forensic Applications

**Industrial Hygiene (Volume 6)**

Metals in Blood and Urine: Biological Monitoring for Worker Exposure • Surface and Dermal Monitoring

**Petroleum and Liquid Fossil Fuels Analysis (Volume 8)**

Metals, Nitrogen and Sulfur in Petroleum Residue, Analysis of

**Steel and Related Materials (Volume 10)**

Atomic Absorption and Emission Spectrometry, Solution-based in Iron and Steel Analysis • Metal Analysis, Sampling and Sample Preparation in

**Atomic Spectroscopy (Volume 11)**

Atomic Spectroscopy: Introduction

**REFERENCES**

1. C.B. Boss, K.J. Fredeen, *Concept, Instrumentation and Techniques in Inductively Coupled Plasma Optical Emission Spectrometry*, 2nd edition, Perkin-Elmer, Norwalk, CT, 1997.
2. J.M. Carey, J.A. Caruso, 'Electrothermal Vaporization for Sample Introduction in Plasma Source Spectrometry', *Crit. Rev. Anal. Chem.*, **23**(5), 397–439 (1992).
3. Leeman Labs, Inc., Hudson, NH, 1999.
4. R.H. Wendt, V.A. Fassel, 'Induction-coupled Plasma Spectrometric Excitation Source', *Anal. Chem.*, **37**(7), 920–922 (1965).
5. S. Greenfield, I.L. Jones, C.T. Berry, 'High-pressure Plasma as Spectroscopic Emission Sources', *Analyst*, **89**(11), 713–720 (1964).
6. V.A. Fassel, 'Analytical Inductively Coupled Plasma Spectroscopies – Past, Present, and Future', *Fresenius Z. Anal. Chem.*, **324**(6), 511–518 (1986).
7. S.R. Koirtiyohann, J.S. Jones, C.P. Jester, D.A. Yates, 'Use of Spatial Emission Profiles and a Nomenclature System as Acids in Interpreting Matrix Effects in the Low-power Argon Inductively Coupled Plasma', *Spectrochim. Acta*, **36B**(1), 49–59 (1981).
8. T. Nakahara, 'Hydride Generation Techniques and Their Applications in Inductively Coupled Plasma–Atomic Emission Spectrometry', *Spectrochim. Acta Rev.*, **14**(1/2), 95–109 (1991).
9. R.E. Russo, 'Laser Ablation', *Appl. Spectrosc.*, **49**(9), 14A–28A (1995).
10. R.S. Babington, 'It's Superspray', *Popular Science*, May, 102–104 (1973).
11. J.G. Williams, 'Instrument Options', in *Inductively Coupled Plasma Mass Spectrometry*, eds. K.E. Jarvis, A.L. Gray, R.S. Houk, Blackie, New York, 58–80, 1992.
12. K. Levine, K.A. Wagner, B.T. Jones, 'Low-cost, Modular Electrothermal Vaporization System for Inductively Coupled Plasma Atomic Emission Spectrometry', *Appl. Spectrosc.*, **52**(9), 1165–1171 (1998).
13. G.M. Allen, D.M. Coleman, 'Segregated Sampling and Excitation with a Dual Inductively Coupled Plasma', *Anal. Chem.*, **56**(14), 2981–2983 (1984).
14. V. Karanassios, K.P. Bateman, 'Electrically Heated Wire-loop, In-torch Vaporization Sample Introduction System for Inductively Coupled Plasma Atomic Emission Spectrometry with Photodiode Array Detection', *Spectrochim. Acta*, **49B**(9), 847–865 (1994).
15. R. Lobinski, F.C. Adams, 'Speciation Analysis by Gas Chromatography with Plasma Source Spectrometric Detection', *Spectrochim. Acta*, **52B**(13), 1865–1903 (1997).
16. S.J. Hill, M.J. Bloxham, P.J. Worsfold, 'Chromatography Coupled with Inductively Coupled Plasma Atomic Emission Spectrometry and Inductively Coupled Plasma Mass Spectrometry', *J. Anal. At. Spectrom.*, **8**(6), 499–515 (1993).
17. T. Kato, T. Uehiro, A. Yasuhara, M. Morita, 'Determination of Methylmercury Species by Capillary Column Gas Chromatography with Axially Viewed Inductively Coupled Plasma Atomic Emission Spectrometric Detection', *J. Anal. At. Spectrom.*, **7**(2), 15–18 (1992).
18. T.S. Conner, J. Yang, J.A. Koropchak, 'New Developments in Thermospray Sample Introduction for Atomic Spectrometry', *Spectrochim. Acta*, **52B**(8), 1087–1104 (1997).
19. V. Karanassios, G. Holick, 'Direct Sample Insertion Devices for Inductively Coupled Plasma Spectrometry', *Spectrochim. Acta Rev.*, **13**(2), 89–166 (1990).
20. L. Moenke-Blankenburg, 'Laser-ICP-spectrometry', *Spectrochim. Acta Rev.*, **15**(1), 1–38 (1993).
21. F.E. Lichte, S.R. Koirtiyohann, 'Induction Coupled Plasma Emission from a Different Angle', Paper 26, Federation of Analytical Chemistry and Spectroscopy Society, Philadelphia, PA, 1976.
22. D.R. Demers, 'Evaluation of the Axially Viewed (End-on) Inductively Coupled Argon Plasma Source for

- Atomic Emission Spectrometry', *Appl. Spectrosc.*, **33**(6), 584–591 (1979).
23. E.C.C. Bailey, *Spectroscopy*, Longman, Green and Co., London, Chapter 1, 1905.
  24. C.W. Earle, M.E. Baker, M. Bonner Denton, R.S. Pomeroy, 'Imaging Applications for Chemical Analysis Utilizing Charge Coupled Device Array Detectors', *Trends Anal. Chem.*, **12**(10), 395–403 (1993).
  25. A.T. Zander, R.L. Chien, C.B. Cooper, P.V. Wilson, 'An Image Mapped Detector for Simultaneous ICP-AES', *Anal. Chem.*, **71**(16), 3332–3340 (1999).
  26. J.M. Mermet, E. Poussel, 'ICP Emission Spectrometers: 1995 Analytical Figures of Merit', *Appl. Spectrosc.*, **49**(10), 12A–18A (1995).
  27. G.L. Long, J.D. Winefordner, 'Limit of Detection: A Closer Look at the IUPAC Definition', *Anal. Chem.*, **55**(7), 712A–724A (1983).
  28. P.W.J.M. Boumans, 'Detection Limits and Spectral Interferences in Atomic Emission Spectrometry', *Anal. Chem.*, **66**(8), 459A–467A (1994).
  29. M. Thompson, R.M. Barnes, 'Analytical Performance of Inductively Coupled Plasma–Atomic Emission Spectrometry', in *Inductively Coupled Plasma in Analytical Atomic Spectrometry*, 2nd edition, eds. A. Montaser, D.W. Golightly, VCH Publishers, New York, 249–297, 1992.
  30. T.C. Johnson, R.S. Perry, L.J. Fick, H.B. Fannin, 'An Examination of Relative Trends of Atomic Detection Limits in the Inductively Coupled Plasma', *Spectrochim. Acta*, **52B**(1), 125–129 (1997).
  31. *The Guide to Techniques and Applications for Atomic Spectroscopy*, Perkin-Elmer, Norwalk, CT, 1990.
  32. W. Slavin (ed.), *Graphite Furnace AAS: A Source Book*, Perkin-Elmer, Ridgefield, CT, 1984.
  33. M. Carre, S. Excoffier, J.M. Mermet, 'A Study of the Relation between the Limit of Detection and the Limit of Quantitation in Inductively Coupled Plasma Spectrochemistry', *Spectrochim. Acta*, **52B**(14), 2043–2049 (1997).
  34. P.J. Galley, G.M. Hieftje, 'Easily Ionizable Element (EIE) Interference in Inductively Coupled Plasma Atomic Emission Spectrometry-II. Minimization of EIE Effects by Choice of Observation Volume', *Spectrochim. Acta*, **49B**(7), 703–724 (1994).